AUTHOR QUERY FORM

AIP Publishing	**Journal: J. Appl. Phys.** **Article Number: 068429JAP**	**Please provide your responses and any corrections by annotating this PDF and uploading it according to the instructions provided in the proof notification email.**

Dear Author,

Below are the queries associated with your article; please answer all of these queries before sending the proof back to AIP.
Please indicate the following:
Figures that are to appear as color online only (i.e., Figs. 1, 2, 3) ______________________ (this is a free service).
Figures that are to appear as color online and color in print ______________________ (a fee of $325 per figure will apply).

Article checklist: In order to ensure greater accuracy, please check the following and make all necessary corrections before returning your proof.

1. Is the title of your article accurate and spelled correctly?
2. Are the author names in the proper order and spelled correctly?
3. Please check affiliations including spelling, completeness, and correct linking to authors.
4. Did you remember to include acknowledgment of funding, if required, and is it accurate?

Location in article	Query / Remark: click on the Q link to navigate to the appropriate spot in the proof. There, insert your comments as a PDF annotation.
AQ1	Please check the edit made in affiliations 1 and 3.
AQ2	Please check the section hierarchy.
AQ3	Refs. 23 and 25 contain identical information. Please check and provide the correct reference or delete the duplicate reference. If the duplicate is deleted, renumber the reference list as needed and update all citations in the text.

Thank you for your assistance.

JOURNAL OF APPLIED PHYSICS **116**, 000000 (2014)

Influence of the substrate choice on the $L1_0$ phase formation of post-annealed Pt/Fe and Pt/Ag/Fe thin films

I. A. Vladymyrskyi,[1,a)] M. V. Karpets,[2] G. L. Katona,[3] D. L. Beke,[3] S. I. Sidorenko,[1] T. Nagata,[4] T. Nabatame,[4] T. Chikyow,[4] F. Ganss,[5] G. Beddies,[5] M. Albrecht,[5,6] and I. M. Makogon[1]

[1]*Metal Physics Department, National Technical University of Ukraine "KPI," Prospect Peremogy 37, 03056 Kyiv, Ukraine*
[2]*I. Frantsevich Institute for Problems of Materials Science, National Academy of Sciences of Ukraine, 3 Krzhizhanovsky Str., 03142 Kyiv, Ukraine*
[3]*Department of Solid State Physics, University of Debrecen, P.O. Box 2, H-4010 Debrecen, Hungary*
[4]*MANA Foundry and MANA Advanced Device Materials Group, National Institute for Materials Science, 1-1 Namiki, Tsukuba 305-0044, Japan*
[5]*Institute of Physics, Chemnitz University of Technology, D-09107 Chemnitz, Germany*
[6]*Institute of Physics, University of Augsburg, Universitätsstraße 1, D-86159 Augsburg, Germany*

(Received 29 May 2014; accepted 16 July 2014; published online xx xx xxxx)

Pt/Fe and Pt/Ag/Fe layered films were deposited by DC magnetron sputtering on MgO(001), $SrTiO_3$(001), and Al_2O_3(0001) single crystalline substrates at room temperature. The films were post-annealed between 623 K and 1173 K for 30 s in flowing N_2 atmosphere. The onset of the $L1_0$-FePt phase formation in films deposited on MgO(001) and $SrTiO_3$(001) substrates was observed after annealing between 773 and 873 K, while chemical $L1_0$ ordering sets in for Pt/Fe bilayers on Al_2O_3(0001) at lower temperatures accompanied by strong (001)-texture. It is concluded that elastic stress, arising from the difference in thermal expansion coefficients between film and substrate, promotes ordering and texture formation.
[http://dx.doi.org/10.1063/1.4891477]

I. INTRODUCTION

FePt thin films have attracted considerable attention as potential ultra-high density magnetic recording material because of the high magneto-crystalline anisotropy of the chemically ordered $L1_0$-FePt phase.[1–5] These films also show high saturation magnetization and excellent corrosion resistance.[6] Typically, the $L1_0$-FePt phase forms from the disordered $A1$-FePt phase after post-annealing or after deposition onto heated substrates. However, industrial application of FePt thin films requires chemical ordering at low temperatures and the control of grain size and orientation.[2,6–8] The ordering temperature can be reduced by Fe/Pt multilayer deposition followed by post-annealing[9,10] or by introducing third elements such as Ag, Au, and Cu.[11–16] A pronounced (001)-texture in $L1_0$-FePt films can be achieved by epitaxial growth at elevated temperatures on single crystalline substrates such as MgO(001)[17–19] or $SrTiO_3$(001).[20] Furthermore, elastic stress during rapid thermal annealing of FePt films on suitable substrates is the origin of strain favoring the growth of (001)-oriented grains in $L1_0$ ordered films.[8,21,22]

In this study, the influence of various single crystalline substrates (MgO(001), $SrTiO_3$(001), and Al_2O_3(0001)) on the structural properties of post-annealed Pt/Fe and Pt/Ag/Fe thin films was investigated using various techniques, including secondary neutral mass spectrometry (SNMS). It is expected that differences in the structural properties of the films after post-annealing arise from the stress created by the difference in thermal expansion coefficients of the metallic film and the substrates (Al_2O_3(0001): 10×10^{-6} K^{-1}, $SrTiO_3$(001): 9.4×10^{-6} K^{-1}, and MgO(001): 5×10^{-6} K^{-1} (Ref. 8)).

II. EXPERIMENTAL

Layered films of Pt(15 nm)/Ag(0; 10 nm)/Fe(15 nm) were deposited at room temperature on MgO(001), $SrTiO_3$(001), and Al_2O_3(0001) single crystalline substrates by DC magnetron sputtering using individual Pt, Ag, and Fe targets. The Ar pressure in the sputtering chamber was adjusted to 0.48 Pa for all depositions. The nominal thicknesses of the layers were evaluated from the sputtering time (determined from the calibrated deposition rate of each target) and verified by profiler measurements. Post-annealing of the films up to 1173 K was carried out in flowing N_2 atmosphere (with 0.2 l/min flowing speed) for 30 s, using a constant heating rate of 10 K/s. The structure of the films was analyzed with an x-ray diffractometer (XRD) equipped with 2-dimensional (2D) and scintillation detectors using Cu K_α radiation. Composition-time (depth) profiles of post-annealed samples were determined by SNMS, using a low-pressure radio-frequency Ar plasma both as source for ion bombardment and as post-ionization medium.[23,24] Furthermore, the magnetic properties were measured by superconductive quantum interference device-vibrating sample magnetometry (SQUID-VSM).

III. RESULTS

A. Pt/Fe and Pt/Ag/Fe films on MgO(001)

Fig. 1 shows 2D XRD images of Pt/Fe and Pt/Ag/Fe films sputter-deposited on MgO(001) substrates after post-annealing

a)Author to whom correspondence should be addressed. Electronic mail: vladymyrskyi@kpm.kpi.ua.

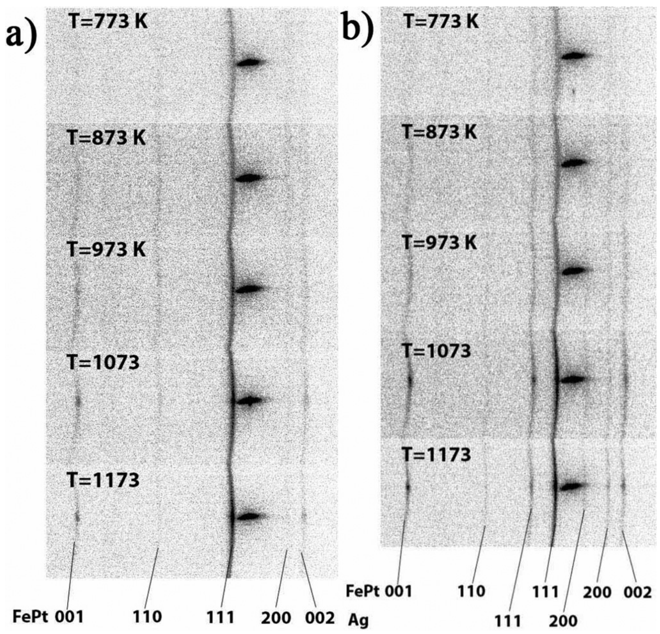

FIG. 1. 2D-XRD images of (a) Pt/Fe and (b) Pt/Ag/Fe films on MgO(001) substrates after post-annealing at different temperatures.

at various temperatures. The appearance of the (001) superstructure peak for both Pt/Fe and Pt/Ag/Fe films was weakly indicated after annealing at 773 K but clearly observed after annealing at 873 K, indicating the onset of the $L1_0$-FePt phase formation. With increasing annealing temperature, this reflection increases in intensity and becomes sharper. However, the intensity of the (111) peak is still much higher than the intensity of (001) reflection, indicating the presence of strong (111)-texture. Furthermore, the intensity of the (111) Ag reflection observed for the Pt/Ag/Fe films also becomes more pronounced with increasing temperature. Please note that it is well known that FePt films grown on MgO(001) substrates at elevated temperatures reveal high $L1_0$ ordering with pronounced (001) texture.[6] However, in our case, the ordering mechanism is quite different as bilayer Fe/Pt films were deposited at room temperature and then post-annealed. Thus, FePt ordering is initiated in the Fe/Pt bilayer apart from the substrate.

SNMS composition profiles versus sputtering time of Pt/Fe and Pt/Ag/Fe films after post-annealing at 773 K and 873 K are presented in Fig. 2. Please note that the composition profile was calculated assuming a linear dependence of the measured intensities on the elemental concentration.[25] Post-annealing of the Pt/Fe film at 773 K leads to an almost homogeneous intermixing between the Pt and Fe layers. Further increase of the temperature up to 873 K does not change significantly the concentration profile. Post-annealing of the Pt/Ag/Fe film at 773 K also leads to the formation of a homogeneous FePt layer and to a moderate penetration of Ag into the FePt layer with an Ag rich layer on the top surface. Please note that from the individual Fe and Pt layer thicknesses, a composition of $Fe_{57}Pt_{43}$ is expected.

B. Pt/Fe and Pt/Ag/Fe films on $SrTiO_3(001)$

Fig. 3 shows 2D XRD images of Pt/Fe and Pt/Ag/Fe films sputter-deposited on $SrTiO_3(001)$ substrates after post-annealing at temperatures up to 1173 K. Please note that the (100) reflection of the $SrTiO_3$ substrate and the (001) reflection of $L1_0$-FePt are superimposed and cannot be easily distinguished. However, the onset of $L1_0$ chemical ordering was registered after post-annealing between 773 K and 873 K in both Pt/Fe and Pt/Ag/Fe films. Intensity of superstructure reflection becomes stronger with higher annealing temperatures. It is apparent that after post-annealing at 1073 K and 1173 K, a non-uniform distribution of the (001) peak intensity along the diffraction ring is observed, revealing that some part of the grains are preferentially oriented along the [001] direction. But the strong (111) peak is still present in the XRD images.

The SNMS depth profiles of post-annealed films grown on $SrTiO_3(001)$ substrates (Fig. 4) are very similar to the

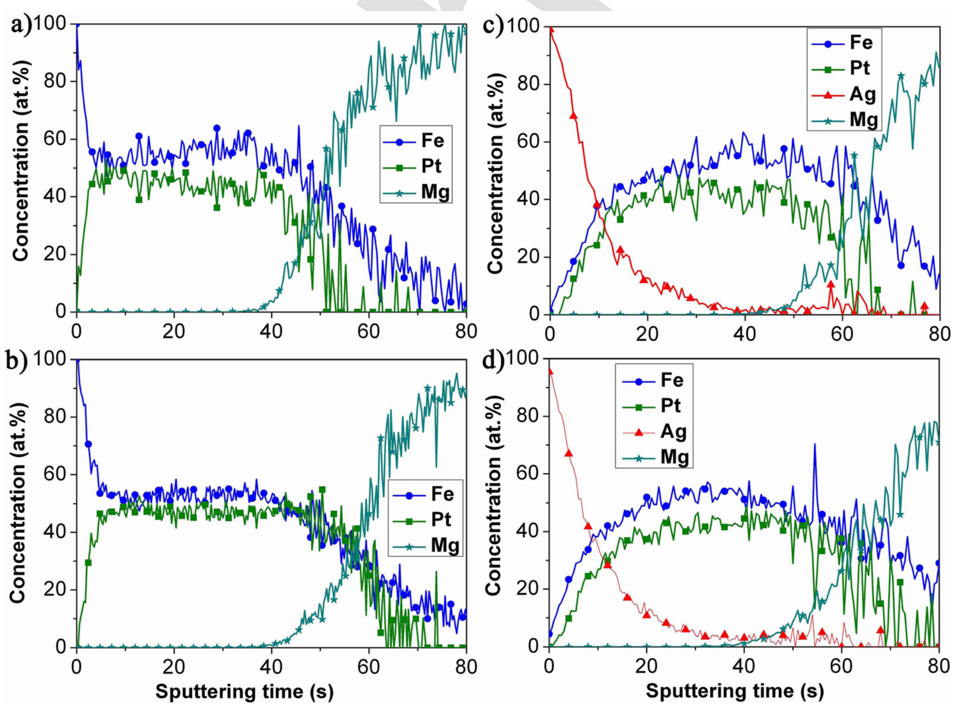

FIG. 2. Composition profiles of films on MgO(001) substrates after post-annealing at 773 K and 873 K: (a) Pt/Fe (773 K); (b) Pt/Fe (873 K); (c) Pt/Ag/Fe (773 K); and (d) Pt/Ag/Fe (873 K).

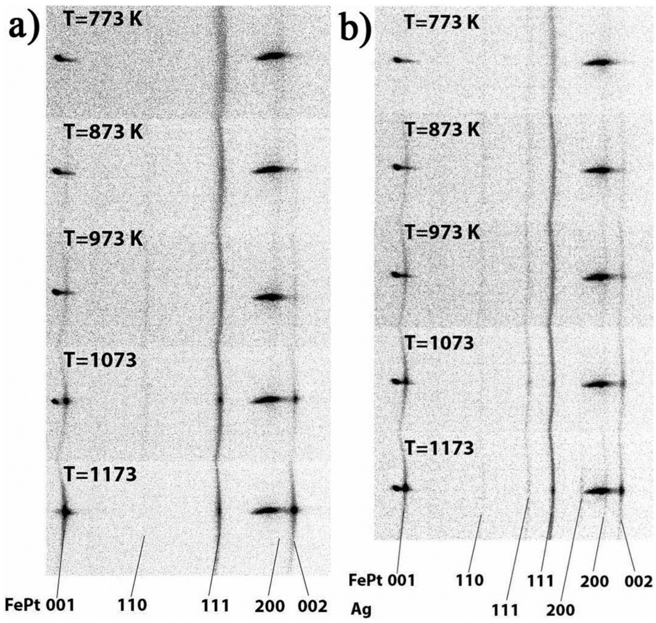

FIG. 3. 2D-XRD images of (a) Pt/Fe and (b) Pt/Ag/Fe films on $SrTiO_3$(001) substrates after post-annealing at different temperatures.

profiles obtained on MgO(001) substrates. Also in this case, annealing at 773 K leads to almost full intermixing between the Fe and Pt layers. Increase of the annealing temperature does not lead to significant changes in the composition distribution. Annealing of films with Ag intermediate layer causes again a moderate penetration of Ag into the FePt layer and segregation towards the free surface.

C. Pt/Fe and Pt/Ag/Fe films on Al_2O_3(0001)

Fig. 5 shows the 2D XRD images of Pt/Fe and Pt/Ag/Fe films sputter-deposited on Al_2O_3(0001) substrates after post-annealing at various temperatures. It is apparent that the (001) superstructure peak is present on the XRD images even after annealing at 773 K for both the Pt/Fe and Pt/Ag/Fe films. These peaks have low intensity as compared to the fundamental (111) reflection, but the intensity is not uniformly distributed along the diffraction ring and has a well defined maximum on the equatorial line, indicating the onset of (001)-texture formation. Additional XRD measurements showed the appearance of the low intensity (001) reflection for the Pt/Fe film after post-annealing at 623 K and for the Pt/Ag/Fe film after post-annealing at 673 K (Fig. 6). The intensity of the (001) reflection increases drastically with increasing annealing temperature, confirming the pronounced (001)-texture for samples post-annealing at 1073 K, which is slightly less pronounced in Pt/Ag/Fe films. However, in Pt/Ag/Fe, a strong (111) reflection remains.

Fig. 7 shows the corresponding SNMS concentration depth profiles of the Pt/Fe and Pt/Ag/Fe films after post-annealing at 773 K and 873 K. The results are very similar to those obtained for films deposited on MgO(001) and $SrTiO_3$(001) substrates. Even after annealing at 773 K, there is an almost homogeneous distribution of Pt and Fe in the Fe/Pt film. Increase of the annealing temperature does not lead to a substantial modification of the concentration profile. For the Pt/Ag/Fe film, full intermixing of the Fe and Pt layers with pronounced Ag surface segregation after post-annealing at 773 K was obtained.

The structural analysis of FePt films formed on Al_2O_3(0001) after post-annealing revealed $L1_0$ ordering and a pronounced (001)-texture, thus a strong perpendicular magnetic anisotropy might be expected in these films. The magnetic properties of the annealed films were investigated by SQUID-VSM. M-H hysteresis loops were measured at room temperature in two geometries: magnetic field is applied in the film plane and out of the film plane. Figure 8 shows normalized M-H hysteresis loops obtained for Pt/Fe and Pt/Ag/Fe films after post-annealing at high temperatures

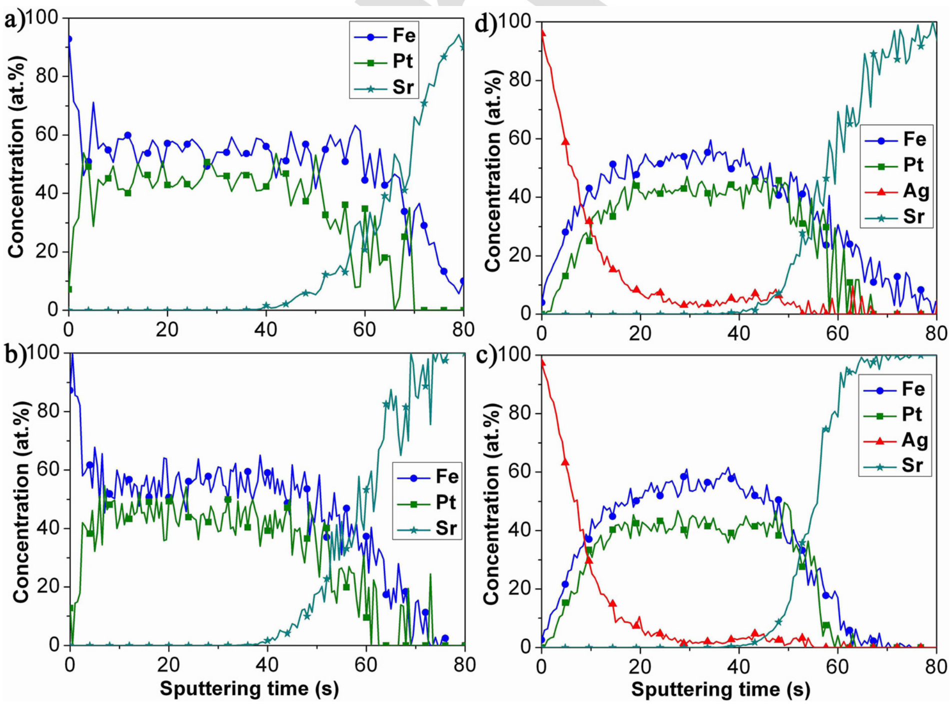

FIG. 4. Composition profiles of films on $SrTiO_3$(001) substrates after post-annealing at 773 K and 873 K: (a) Pt/Fe (773 K); (b) Pt/Fe (873 K); (c) Pt/Ag/Fe (773 K); and (d) Pt/Ag/Fe (873 K).

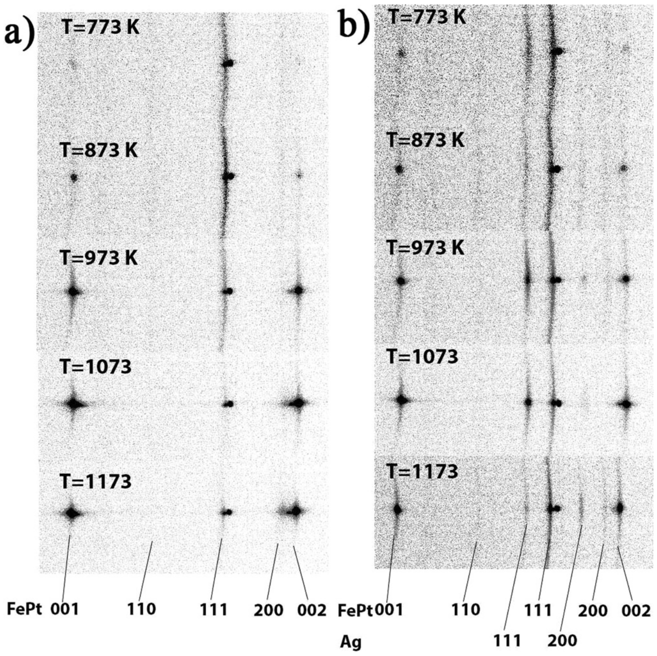

FIG. 5. 2D-XRD images of (a) Pt/Fe and (b) Pt/Ag/Fe films on $Al_2O_3(0001)$ substrates after post-annealing at different temperatures.

(973 K–1073 K). The magnetization curves for all films are quite similar and a more or less isotropic behavior in magnetization reversal for the in-plane and out-of-plane field directions is observed. The coercivity of the Pt/Fe films after post-annealing at 973 K and 1073 K is 14.0 kOe and 15.8 kOe, respectively. For films with Ag intermediate layer, these values were increased up to 17.7 kOe and 24.2 kOe, respectively. This behavior can be explained by Ag diffusion to the grain boundaries, which results in exchange decoupling of FePt grains, which in turn enhances the coercivity. Furthermore, the still present (111) and (200) orientations are responsible for the isotropic magnetic properties due to the rather randomly oriented FePt grains.

XRD results presented above indicate that the deposition of Pt/Fe and Pt/Ag/Fe layered films onto single crystalline $Al_2O_3(0001)$ substrates with hexagonal structure leads to decrease of the $L1_0$-FePt phase formation temperature as compared to MgO(001) and $SrTiO_3(001)$ substrates with cubic lattice. Moreover, annealing of the films on $Al_2O_3(0001)$ substrate results in pronounced (001)-texture formation. On the other hand, introduction of the Ag intermediate layer leads to the slight deterioration of the (001)-texture with the presence of a strong (111) reflection. Results of the SNMS depth profiling were very similar for films sputtered onto the all investigated single crystalline substrates: even after post-annealing at 773 K almost homogeneous intermixing of the Pt and Fe layers was observed. This fact indicates that there is no noticeable effect of the substrate type on the diffusion processes but its influence on the chemical ordering and texture formation is more significant.

The Ag intermediate layer increases the coercivity of the films after their post-annealing. This can be explained by decreasing the magnetic interaction between the $L1_0$-FePt grains due to their isolation. Isolated grains were formed because of the limited Ag solubility in FePt lattice and its grain boundary and surface segregation tendency (as was shown above). This conclusion is in agreement with the conclusions obtained in Ref. 26. Despite the pronounced (001)-texture, films deposited onto $Al_2O_3(0001)$ substrates are magnetically isotropic, indicating the presence of chemically disordered A1 grains and $L1_0$ ordered grains with (111) and (200) orientations.

The observed differences in the texture formation in the films deposited onto different substrates can be explained by

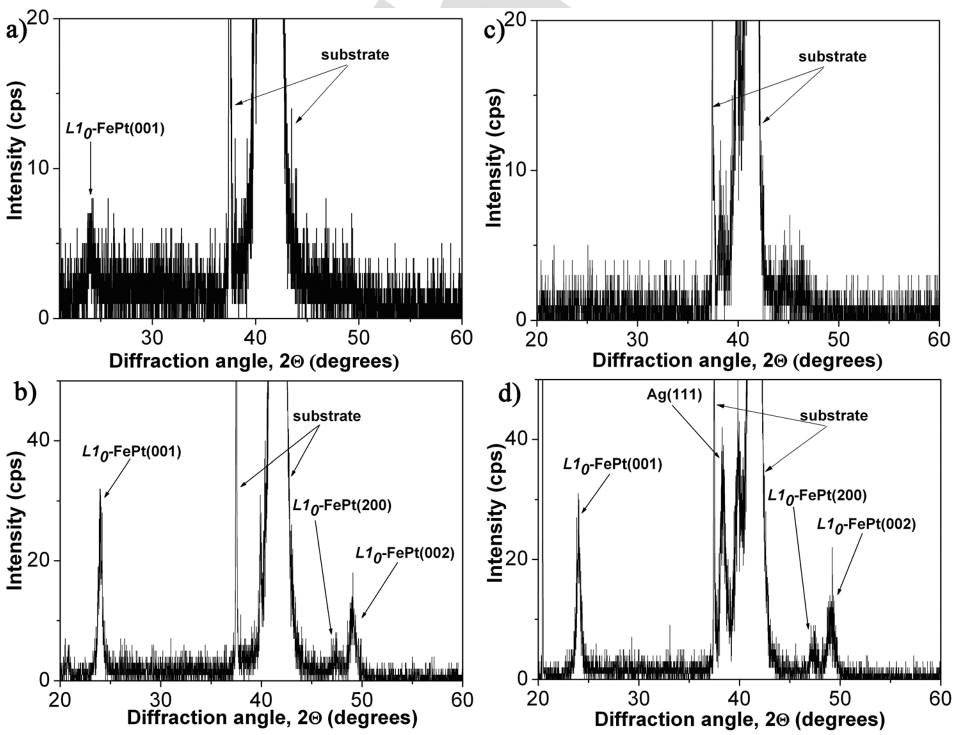

FIG. 6. XRD (Θ-2Θ)-scans of film samples deposited on $Al_2O_3(0001)$ substrates after post annealing at different temperatures: (a) Pt/Fe at 623 K; (b) Pt/Fe at 673 K; (c) Pt/Ag/Fe at 623 K; and (d) Pt/Ag/Fe at 673 K.

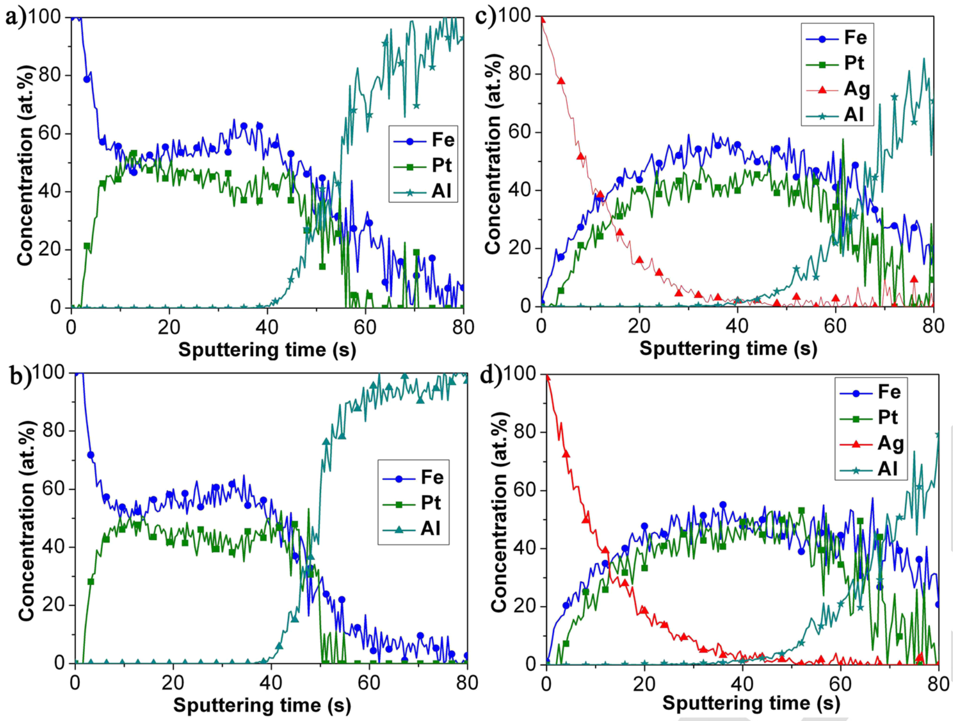

FIG. 7. Composition profiles of films on Al_2O_3(0001) substrates after post-annealing at different temperatures: (a) Pt/Fe at 773 K; (b) Pt/Fe at 873 K; (c) Pt/Ag/Fe at 773 K; and (d) Pt/Ag/Fe at 873 K.

stresses, created by the mismatch between crystal lattices and by the difference of the thermal expansion coefficients of metallic layers and the substrate. These stresses are the origin of the strain favoring the growth of [001]-oriented grains.[22] Stresses arising due to the difference in thermal expansion coefficients can be calculated from the equation[27]

$$\sigma = \Delta\alpha\Delta T E/(1-\mu),$$

where $\Delta\alpha$ is the difference in the thermal expansion coefficients between the substrate and the film, ΔT is the temperature difference between room and the post-annealing temperatures, E is the elastic modulus of the film, and μ is Poisson's ratio. As the elastic modulus is temperature dependent, and in our case the Fe layer interacts with the Pt, forming first $A1$-FePt and then $L1_0$-FePt phases, we used the elastic modulus (180 GPa), Poisson's ratio (0.33), and thermal expansion coefficient ($10.5 \times 10^{-6}\ K^{-1}$) for bulk FePt for the estimation of the difference in the stresses occurring in the films deposited onto different substrates. Fig. 9 shows the calculated stresses that arise from thermal expansion mismatch as a function of temperature for the investigated samples. It is clear that the level of compressive stresses in the films deposited onto Al_2O_3(0001) substrates is much higher as compared to MgO(001) and $SrTiO_3$(001) substrates.

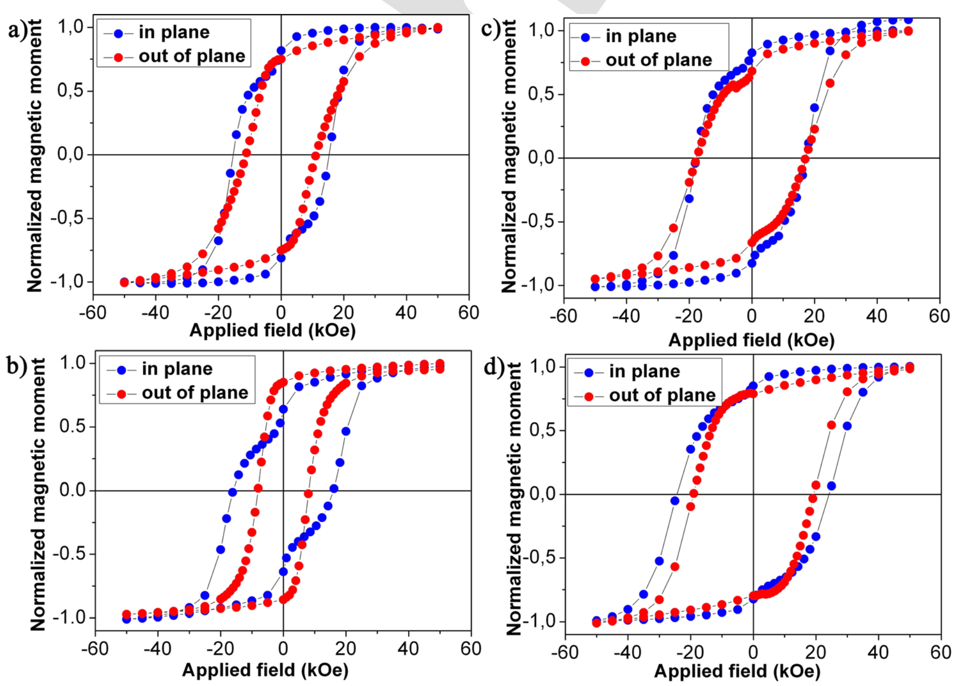

FIG. 8. SQUID-VSM M-H hysteresis loops of films annealed at different temperatures: (a) Pt/Fe at 973 K; (b) Pt/Fe at 1073 K; (c) Pt/Ag/Fe at 973 K; and (d) Pt/Ag/Fe at 1073 K.

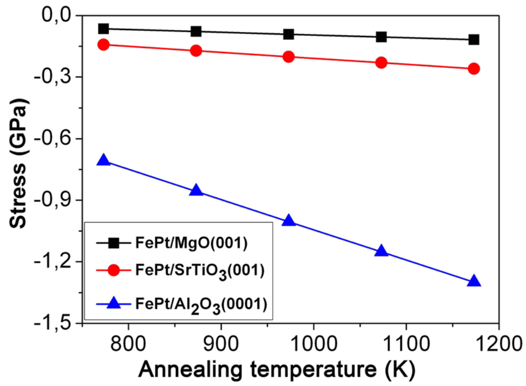

FIG. 9. Calculated thermal stresses arising from differences in thermal expansion coefficient between the substrate and the FePt film.

These stresses promote the chemical ordering and texture formation in the films.

IV. CONCLUSION

In conclusion, sputtering of the Pt/Fe and Pt/Ag/Fe films onto Al_2O_3(0001) single crystalline substrates and following post-annealing leads to the formation of pronounced (001)-texture. Furthermore, the onset temperature for chemical ordering in these films is lower compared to films prepared on MgO(001) and $SrTiO_3$(001) substrates. It is important to note that there is no noticeable effect of the substrate choice on the diffusion process but its influence on the chemical ordering and texture formation is significant. Differences in the structural properties of the films deposited onto different substrates can be explained by the stress state that occurs during post-annealing. Also it was shown that introduction of the Ag intermediate layer is an effective method to increase the coercivity of the film.

ACKNOWLEDGMENTS

This work was financially supported by the Deutsche Akademischer Austauschdienst (DAAD) in the frame of the Leonard-Euler-Program (Grant No. 50744282) and by the Ministry of Education and Science of Ukraine (Grant No. 0212U008249). The research was also supported by the TÁMOP-4.2.2.A-11/1/KONV-2012-0036 project, implemented through the New Hungary Development Plan co-financed by the European Social Fund, and the European Regional Development Fund. The authors gratefully acknowledge the support of the Hungarian Scientific Research Fund (OTKA) through Grant No. NF 101329. This research was also supported by the European Union and the State of Hungary, co-financed by the European Social Fund in the framework of the TÁMOP 4.2.4. A/2-11-1-2012-0001 "National Excellence Program" (author G. L. Katona).

[1]D. Weller, O. Mosendz, G. Parker, S. Pisana, and T. S. Santos, "$L1_0$ FePtX–Y media for heat-assisted magnetic recording," Phys. Status Solidi A **210**, 1245 (2013).
[2]*Development in Data Storage, Materials Perspective*, edited by S. N. Piramanayagam and T. C. Chong (John Wiley & Sons, Inc., New York, 2012).
[3]A. T. McCallum, P. Krone, F. Springer, C. Brombacher, M. Albrecht, E. Dobisz, M. Grobis, D. Weller, and O. Hellwig, "$L1_0$ FePt based exchange coupled composite bit patterned films," Appl. Phys. Lett. **98**, 242503 (2011).
[4]L. Zhang, Y. K. Takahashi, A. Perumal, and K. Hono, "$L1_0$ FePt ordered high coercivity (FePt)Ag-C granular thin films for perpendicular recording," J. Magn. Magn. Mater. **322**, 2658–2664 (2010).
[5]T. Bulat and D. Goll, "Large-area hard magnetic $L1_0$-FePt nanopatterns by nanoimprint lithography," Nanotechnology **22**, 315301 (2011).
[6]J. Lyubina, B. Rellinghaus, O. Gutfleisch, and M. Albrecht, in *Handbook of Magnetic Materials*, edited by K. H. J. Buschow (Elsevier, Amsterdam, 2011), Vol. 19, pp. 291–395.
[7]Y. K. Takahashi and K. Hono, "On low-temperature ordering of FePt films," Scr. Mater. **53**, 403 (2005).
[8]P. Rasmussen, X. Rui, and J. E. Shield, "Texture formation in FePt thin films via thermal stress management," Appl. Phys. Lett. **86**, 191915 (2005).
[9]M. L. Yan, N. Powers, and D. J. Sellmyer, "Highly oriented nonepitaxially grown $L1_0$ FePt films," J. Appl. Phys. **93**, 8292 (2003).
[10]Y. C. Wu, L. W. Wang, and C. H. Lai, "Low-temperature ordering of (001) granular FePt films by inserting ultrathin SiO_2 layers," Appl. Phys. Lett. **91**, 072502 (2007).
[11]Y. S. Yu, H.-B. Li, W. L. Li, M. Liu, and W. D. Fei, "Low-temperature ordering of $L1_0$ FePt phase in FePt thin film with AgCu underlayer," J. Magn. Magn. Mater. **320**, L125 (2008).
[12]C. Feng, Q. Zhan, B. Li, J. Teng, M. Li, Y. Jiang, and G. Yu, "Magnetic properties and microstructure of FePt/Au multilayers with high perpendicular magnetocrystalline anisotropy," Appl. Phys. Lett. **93**, 152513 (2008).
[13]Y. S. Yu, H.-B. Li, W. L. Li, M. Liu, and W. D. Fei, "Structure and magnetic properties of magnetron sputtered $[(Fe/Pt/Fe)/Au]_n$ multilayer films," J. Magn. Magn. Mater. **322**, 1770 (2010).
[14]W. Y. Zhang, H. Shima, F. Takano, H. Akinaga, X. Z. Yu, T. Hara, W. Z. Zhang, K. Kimoto, Y. Matsui, and S. Nimori, "Enhancement in ordering of $Fe_{50}Pt_{50}$ film caused by Cr and Cu additives," J. Appl. Phys. **106**, 033907 (2009).
[15]C. Feng, B.-H. Li, Y. Liu, J. Teng, M.-H. Li, Y. Jiang, and G.-H. Ya, "Improvement of magnetic property of $L1_0$-FePt film by FePt/Au multi-layer structure," J. Appl. Phys. **103**, 023916 (2008).
[16]O. P. Pavlova, T. I. Verbitska, I. A. Vladymyrskyi, S. I. Sidorenko, G. L. Katona, D. L. Beke, G. Beddies, M. Albrecht, and I. M. Makogon, "Structural and magnetic properties of annealed FePt/Ag/FePt thin films," Appl. Surf. Sci. **266**, 100 (2013).
[17]R. F. C. Farrow, D. Weller, R. F. Marks, M. F. Toney, A. Cebollada, and G. R. Harp, "Control of the axis of chemical ordering and magnetic anisotropy in epitaxial FePt films," J. Appl. Phys. **79**, 5967 (1996).
[18]Y. K. Takahashi and K. Hono, "Interfacial disorder in the $L1_0$ FePt particles capped with amorphous Al_2O_3," Appl. Phys. Lett. **84**, 383 (2004).
[19]T. Bulat and D. Goll, "Temperature dependence of the magnetic properties of $L1_0$-FePt nanostructures and films," J. Appl. Phys. **108**, 113910 (2010).
[20]Y. F. Ding, J. S. Chen, and E. Liu, "Epitaxial $L1_0$ FePt films on $SrTiO_3$(100) by sputtering," J. Cryst. Growth **276**, 111 (2005).
[21]M. Albrecht and C. Brombacher, "Rapid thermal annealing of FePt thin films," Phys. Status Solidi A **210**, 1272 (2013).
[22]L.-W. Wang, W.-C. Shih, Y. C. Wu, and C.-H. Lai, "Promotion of [001]-oriented $L1_0$-FePt by rapid thermal annealing with light absorption layer," Appl. Phys. Lett. **101**, 252403 (2012).
[23]H. Oechsner, R. Getto, and M. Kopnarski, "Quantitative characterization of solid state phases by secondary neutral mass spectrometry," J. Appl. Phys. **105**, 063523 (2009). AQ3
[24]L. Péter, G. L. Katona, Z. Berényi, K. Vad, G. A. Langer, E. Tóth-Kádar, J. Pádár, L. Pogány, and I. Bakonyi, "Electrodeposition of Ni–Co–Cu/Cu multilayers: 2. Calculations of the element distribution and experimental depth profile analysis," Electrochim. Acta **53**, 837 (2007).
[25]H. Oechsner, R. Getto, and M. Kopnarski, "Quantitative characterization of solid state phases by secondary neutral mass spectrometry," J. Appl. Phys. **105**, 063523 (2009).
[26]I. A. Vladymyrskyi, O. P. Pavlova, T. I. Verbitska, S. I. Sidorenko, G. L. Katona, D. L. Beke, and I. M. Makogon, "Influence of intermediate Ag layer on the structure and magnetic properties of Pt/Ag/Fe thin films," Vacuum **101**, 33 (2014).
[27]D. Burgreen, *Elements of Thermal Stress Analysis* (C.P. Press, New York, 1971).